

Irreversibility in Non-reciprocal Chaotic Systems

Tuan Pham,¹ Albert Alonso,¹ and Karel Proesmans¹

¹*Niels Bohr Institute, University of Copenhagen,
Blegdamsvej 17, Copenhagen, 2100-DK, Denmark*

How is the irreversibility of a high-dimensional chaotic system controlled by the heterogeneity in the non-reciprocal interactions among its elements? In this paper, we address this question using a stochastic model of *random* recurrent neural networks that undergoes a transition from quiescence to chaos at a critical heterogeneity. In the thermodynamic limit, using dynamical mean field theory, we obtain an exact expression for the averaged entropy production rate – a measure of irreversibility – for any heterogeneity level J . We show how this quantity becomes a constant at the onset of chaos, while changing its functional form upon crossing this point. The latter can be elucidated by closed-form approximations valid for below and slightly above the critical point and for large J .

Introduction. Complex systems of heterogeneously interacting agents are intrinsically out-of-equilibrium. Underlying their emergent behaviours is the intricate interplay between stochasticity, non-linearity and non-reciprocity of interactions. To understand the dynamics of these systems, a general framework known as dynamical mean field theory (DMFT) [1–7] has been developed. Significant progress has been made in a variety of problems through DMFT, including the relaxation of p -spin glasses towards weak ergodicity-breaking states [8], the dynamics of random replicator [9] and the effective noise of stochastic gradient descent [10], to name but a few. A renewed interest in applying DMFT to complex systems, such as neural networks [11–15], ecology [16–19], biological adaptation [20], oscillatory dynamics [21, 22], and active matter [23, 24], has emerged recently.

Meanwhile, the thermodynamics of non-equilibrium phase transitions has been studied in a wide variety of systems, including active matters [25–29], spin models with order-disorder transitions [30–34], other systems with synchronisation transitions [35], Hopf bifurcations [36], the onset of limit cycles [37] and pattern formations [38, 39]. Meanwhile, progress on incorporating a thermodynamic treatment into DMFT has so far been limited to discrete-time systems [40]. A proper understanding of the onset of chaos – one of the most important classes of non-equilibrium phase-transitions, is, to the best of our knowledge, currently lacking.

The goal of this letter is two-fold. On the one hand, we want to integrate stochastic thermodynamics into the DMFT treatment of continuous-time dynamics. This will not only deepen our understanding of the energetic cost associated with operating complex and disordered systems, but also facilitate the applications of general results from stochastic thermodynamics, such as the thermodynamic uncertainty relations [41, 42] and speed-limits [43, 44], to those systems. On the other hand, we aim to build a thermodynamic theory of chaotic systems that can quantify their behaviours using entropy production.

We illustrate these ideas using an important model of random neural networks – sometimes referred to as the “Wilson–Cowan” model [45]. This model has been widely

used to study machine-learning algorithms [46] and, by means of DMFT [47–50], a transition from fixed-point regime to chaos beyond a critical heterogeneity level of synaptic weights has been established. Such a transition is believed to be particularly relevant for understanding the computational capabilities of neural networks with an optimal information processing capacity at the edge of chaos [51, 52] and the cost of this information processing itself [53]. Our work can shed light on the question of how the energy dissipation, as quantified by the entropy production rate, changes at this transition. Though we shall focus on a thermodynamically-consistent model of neural networks, we need to stress that our methodology can be extended to other systems amenable to DMFT analysis, such as active matter and ecological models.

Model. We consider a system of N neurons, each characterized by a continuous variable $x_i(t)$ and has a saturating nonlinear input-output transfer function f . We choose $f(\cdot) = \tanh(\cdot)$. They are coupled through a fully-connected network of interactions \mathbf{J} without self-loop (i.e. $J_{ii} = 0, \forall i$). The dynamics of these units are modelled as Langevin equations,

$$\frac{dx_i}{dt} = -x_i + \tanh\left(\sum_{j=1, j \neq i}^N J_{ij}x_j\right) + \xi_i(t) \quad (1)$$

where $\xi_i(t)$ is a zero-mean white noise with correlator $C_\xi(t, t') \equiv \langle \xi_i(t)\xi_j(t') \rangle_\xi = \sigma^2 \delta_{ij} \delta(t - t')$, which corresponds to a thermal noise from the environment and is related to the environment’s temperature T as $k_B T = \sigma^2/2$, with k_B the Boltzmann constant. Here we consider a *quenched* ensemble of network configurations with asymmetric (i.e. uncorrelated) independent Gaussian couplings J_{ij} , whose mean, variance and covariance are

$$[J_{ij}]_{\mathbf{J}} = \frac{\mu}{N}; [J_{ij}^2]_{\mathbf{J}} = \frac{J^2}{N}; \left[\left(J_{ij} - \frac{\mu}{N} \right) \left(J_{ji} - \frac{\mu}{N} \right) \right]_{\mathbf{J}} = 0 \quad (2)$$

Hereafter $[\cdot]_{\mathbf{J}}$, referred to as ensemble average, denotes averaging with respect to the coupling distribution $P(\mathbf{J}) = \prod_{i \neq j} P(J_{ij})$. In this paper we will consider only the case of $\mu = 0$. The network is then called ‘balanced’,

as each neuron, on average, has a net zero input due to a balance between excitation and inhibition. Though we use Gaussian distributions for the coupling strengths, distributions that include a δ function at zero, corresponding to sparse connections, or that have discrete support, corresponding to a finite number of possible strengths, give the same results in the large N limit [13].

We note that Eq. (1) does not satisfy detailed balance due to the non-reciprocity ($J_{ij} \neq J_{ji}$) and due to the non-linearity of the input-output transfer function. The system is hence out of equilibrium and constantly produces entropy, even in steady state. In the low-noise limit, $\sigma \rightarrow 0$, it exhibits two different phases, namely a disordered phase, where the dynamics evolves to a fixed point, for $J < 1$ and a chaotic phase, for $J > 1$, where all neurons keep fluctuating despite the absence of noise.

Entropy production rate. We want to compute the entropy production rate of the system described in Eqs. (1)-(2), using the following decomposition of the total entropy production rate according to stochastic thermodynamics [54]:

$$\dot{S}_{\text{tot}} = \dot{S}_{\text{res}} + \dot{S}_{\text{sys}}$$

with

$$\dot{S}_{\text{res}} = \frac{2}{\sigma^2} \sum_i F_i(\mathbf{x}) \circ \frac{dx_i}{dt}, \quad F_i(\mathbf{x}) \equiv -x_i + \tanh([\mathbf{J}\mathbf{x}]_i) \quad (3)$$

$$\dot{S}_{\text{sys}} = -k_B \sum_i \left(\frac{\partial}{\partial x_i} \ln p(\mathbf{x}, t) \right) \circ \frac{dx_i}{dt} - k_B \frac{\partial}{\partial t} \ln p(\mathbf{x}, t) \quad (4)$$

the rate at which entropy is dissipated into the environment and the change in systems entropy, respectively. Here “ \circ ” denotes the Stratonovich convention and $p(\mathbf{x}, t)$ is the joint probability distribution of all neurons at time t . At steady state, the average system entropy production rate vanishes, $\langle \dot{S}_{\text{sys}}^{(\text{ss})} \rangle = 0$, and hence $\langle \dot{S}_{\text{tot}}^{(\text{ss})} \rangle = \langle \dot{S}_{\text{res}}^{(\text{ss})} \rangle$, where the $\langle \cdot \rangle$ represent the average taken over all noise-realizations. Therefore, we shall focus on calculating the entropy production in the reservoir, \dot{S}_{res} for the remainder of this paper.

DMFT description. In the $N \rightarrow \infty$ limit, the system is self-averaging, i.e., its macroscopic behaviour can be assumed to depend only on the statistical properties of the disorder in Eq. (2). Using DMFT, we obtain one-dimensional effective dynamics that become an *exact* description of the dynamics Eq. (1) as $N \rightarrow \infty$:

$$\dot{x} = -x(t) + u(t) + \xi(t), \quad u \equiv \tanh(\eta(t)) \quad (5)$$

where we have introduced η – a Gaussian noise with zero mean and whose correlation $C_\eta(t, t') \equiv \langle \eta(t)\eta(t') \rangle$, needs to be defined self-consistently as

$$C_\eta(t, t') = J^2 C_x(t, t') \quad (6)$$

with

$$C_x(t, t') \equiv \langle x(t)x(t') \rangle \quad (7)$$

One can interpret $x(t)$ as the representative neuron of a homogeneous population, in which all neurons with statistically identical connections and dynamical properties become identical after taking the ensemble average. Therefore, we have

$$[\langle x_k(t) \rangle]_{\mathbf{J}} = \langle x(t) \rangle^{(MF)}, \quad \forall k = 1, \dots, N. \quad (8)$$

The superscript (MF) denotes the average taken over the mean-field dynamics Eq. (5). Though Eq. (5) is a linear equation in terms of $x(t)$, the non-linearity of the full system Eq. (1) is encoded in the self-consistency relation Eq. (6) [note the difference with the celebrated model in [47] whose effective dynamics are given by $(\partial_x + 1)x(t) = \eta(t) + \xi(t)$ with $C_\eta(t, t') = J^2 \langle \tanh(x(t))\tanh(x(t')) \rangle$].

In appendix A, we show that this equivalence between the exact and the DMFT dynamics can be extended to the entropy production into the environment,

$$[\langle \dot{S}_{\text{res}}(t) \rangle]_{\mathbf{J}} = \langle \dot{S}_{\text{res}}^{(MF)}(t) \rangle, \quad (9)$$

with $\dot{S}_{\text{res}}(t) = \dot{S}_{\text{res}}(t)/N$ and

$$\dot{S}_{\text{res}}^{(MF)}(t) = (-x(t) + u(t)) \circ \frac{dx(t)}{dt}. \quad (10)$$

We dropped the superscript over the average for notational simplicity. This allows us to conclude that the average entropy flux into the environment per neuron in the original system is exactly the same as that of the DMFT one. Hereafter, we will focus on calculating the average entropy production rate through this DMFT approach.

Before continuing a (semi-)analytical calculation of the entropy production rate, we numerically verify the agreement between simulations of the dynamics Eq. (1) and its DMFT description given in Eq. (5). In Fig. 1 (c)-(d) an excellent agreement between the two dynamics is found for both $C_x(t, t')$ and $\langle \dot{S}_{\text{res}}(t) \rangle$ even before reaching steady states both for the fixed-point dynamics (Fig. 1 (a)) as for the chaotic phase (Fig. 1 (b)).

In appendix B, we show that under the steady-state conditions, for which $C_x(\tau) = \lim_{t' \rightarrow \infty} C_x(t', t' + \tau)$, the entropy production rate simplifies to

$$\langle \dot{S}_{\text{res}}^{(MF)} \rangle = -\frac{2}{\sigma^2} \ddot{C}_x(0^+) + 1, \quad (11)$$

which means that knowledge of the auto-correlation function of a single neuron x obeying Eq. (5) is sufficient to calculate the entropy production rate of the system. According to [13], the curvature $\ddot{C}_x(0^+)$ changes its sign from positive to negative once crossing the *true* critical point J^* , resulting in $\langle \dot{S}_{\text{res}}^{(MF)} \rangle < 1$ and $\langle \dot{S}_{\text{res}}^{(MF)} \rangle > 1$, below and above J^* , respectively. At $J = J^*$, $\ddot{C}_x(0^+) = 0$, yielding

$$\langle \dot{S}_{\text{res}}^{(MF)} \rangle_{J=J^*} = 1 \quad (12)$$

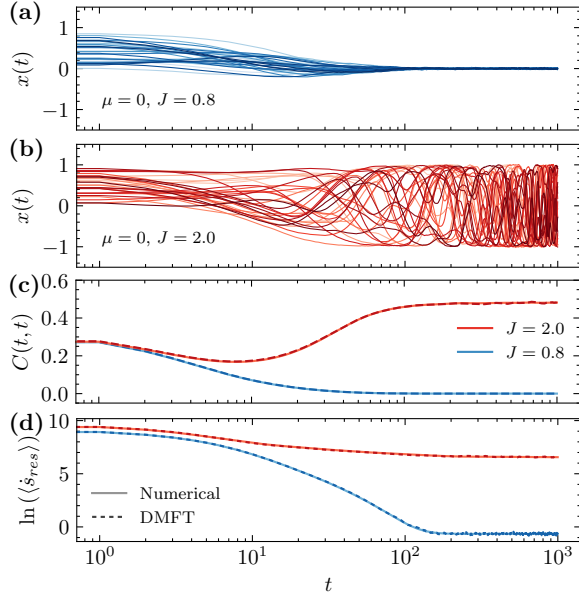


FIG. 1. **(a)-(b)** Time series of neuronal states evolving according to Eq. (1) in the trivial-fixed-point regime ($J = 0.8$); and the chaotic regime ($J = 2$). **(c)-(d)** Equal-time correlation $C(t, t)$ and the entropy production rate for the trivial-fixed-point regime (blue) and in the chaotic regime (red). $N = 1000$ neurons for the numerics and $N_{\text{traj}} = 1000$ trajectories are used for the numerical integration of DMFT. In all panels, $\sigma = 0.01$ and $x(0)$ is uniformly distributed in $[0, 1]$.

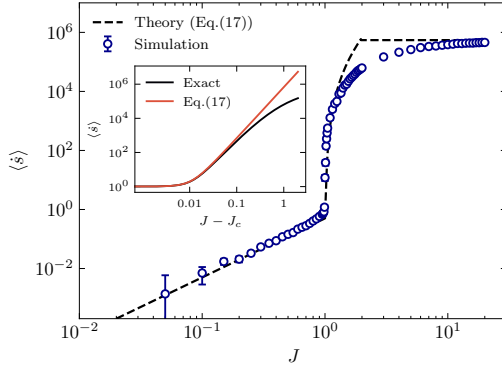


FIG. 2. Comparison of $\langle \dot{s}_{\text{res}}^{\text{(ss)}} \rangle$ from simulations with $\sigma = 0.001$, $N = 1000$ and the asymptotics given by Eq. (17). The inset shows the comparison between the entropy production computed by the exact numerics of DMFT and the asymptotics near $J \approx J_c = 1 + 3^{1/4}\sigma$.

Solution of the DMFT equation. Following the pioneering approach in [47, 48], we map the dynamics of $C_x(\tau)$ onto that of a *classical* particle moving under a potential V parametrized by the initial condition $C_0 \equiv C_x(0)$. As detailed in appendix C, for $\tau \geq 0$, one can write (cf. Appendix C):

$$\partial_\tau^2 C_x(\tau) = -\frac{\partial}{\partial C_x(\tau)} V(C_x(\tau)|C_0) - \sigma^2 \delta(\tau)$$

$$V(C_x(\tau)|C_0) = \frac{\langle \Omega(\eta(0))\Omega(\eta(\tau)) \rangle_\eta - \langle \Omega(\eta(0)) \rangle_\eta^2}{J^2} - \frac{C_x(\tau)^2}{2} \quad (13)$$

where $\Omega(z) := \ln \cosh(z) = \int_0^z \tanh(y) dy$ and

$$\langle \Omega(\eta(0))\Omega(\eta(\tau)) \rangle_\eta = \int \int d\eta_1 d\eta_2 \frac{e^{-\frac{(C_0(\eta_1^2 + \eta_2^2) - 2C_x(\tau)\eta_1\eta_2)}{2J^2(C_0^2 - C_x(\tau)^2)}}}{2\pi J^2 \sqrt{C_0^2 - C_x(\tau)^2}} \Omega(\eta_1)\Omega(\eta_2), \quad (14)$$

and a similar equation for $\langle \Omega(\eta(0)) \rangle_\eta$. One can find C_0 through the following equations:

$$V(C_0|C_0) = -\frac{\sigma^4}{8}, \quad \dot{C}_x(0^+) = -\frac{\sigma^2}{2}. \quad (15)$$

The entropy production rate given in Eq. (11) can also be rewritten in terms of the potential V as

$$\langle \dot{s}_{\text{tot}}^{(MF)} \rangle = \frac{2}{\sigma^2} \frac{\partial}{\partial C_x(\tau)} V(C_x(\tau)|C_0) \Big|_{C_x(\tau)=C_0} + 1. \quad (16)$$

This equation provides a numerical procedure to calculate exactly the entropy production rate of the network in the thermodynamic limit: we use the first one in Eq. (15) to find C_0 , then apply Price's theorem to calculate $V(C_x|C_0)$ by Eq. (13) and finally compute the entropy production rate by Eq. (16). Hereafter we shall refer this procedure as *the exact numerics of DMFT* to distinguish it from the other scheme consisting of numerically integrating the effective dynamics Eq. (5) and computing the associated $\langle \dot{s}_{\text{tot}}^{(MF)} \rangle$ by simulating Eq. (10).

Limits and asymptotics To get more intuition about the entropy production rate, we shall derive a number of analytical results from solutions to the above set of equations in some limits. In appendix D, we show that

$$\langle \dot{s}_{\text{tot}}^{(MF)} \rangle \simeq \begin{cases} \frac{J^2}{2} & J \ll 1 \\ \frac{2}{3\sigma^2} \left[\frac{(J-1)^2}{2} + \frac{1}{2} \sqrt{(J-1)^4 - 3\sigma^4} \right]^{1/2} \sqrt{(J-1)^4 - 3\sigma^4} + 1 & 0 \leq J - J_c \ll 1, \text{ and } \sigma^2 \ll 1, \\ \frac{4}{\pi\sigma^2} \left(1 - \sqrt{\left(1 - \frac{\pi}{2}\right)^2 + \left(\frac{\pi\sigma^2}{4}\right)^2} \right) + 1 & J \gg 1 \end{cases} \quad (17)$$

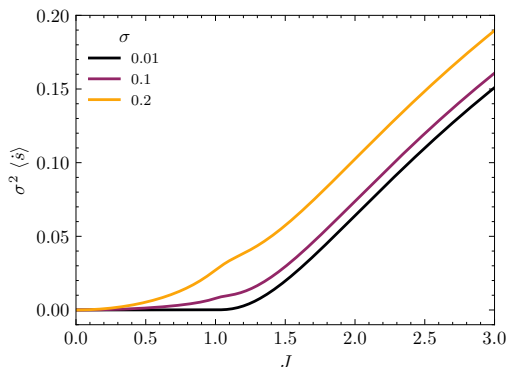


FIG. 3. $\sigma^2 \langle \dot{s}_{\text{tot}}^{(MF)} \rangle$ as a function for J for various choices of σ . One can observe a clear change in the behavior of this quantity around $J \approx 1$, signalling a phase-transition. Here $\langle \dot{s}_{\text{tot}}^{(MF)} \rangle$ is computed using the exact numerics of DMFT.

where in the small-noise limit $J_c = 1 + 3^{1/4}\sigma$. J_c is the lowest order approximation of the true critical point J^* .

We compare our analytical approximation in Eqs. (17) with direct numerical simulations of Eq. (3) at a fixed noise strength $\sigma = 0.001$ in Fig. 2. We verify that $\langle \dot{s}_{\text{tot}} \rangle \approx J^2/2$ up to values relatively close to $J = 1$. Subsequently, the second and third lines of Eq. (17) capture the transition into the chaotic regime. We also find that entropy production rate does indeed level off at the value predicted by the last line of Eq. (17) around $J \approx 10$. The inset shows the comparison between our approximation Eq. (17) of the entropy production rate and its exact calculations obtained from Eqs. (13)-(16) for J near J_c . One can see that our approximation, Eq. (17), is indeed in good agreement with the exact dynamics and that the entropy production goes to 1 as J approaches J_c .

As mentioned in the beginning of this paper, this model exhibits two phases in the low-noise limit, $\sigma \rightarrow 0$: a disordered phase for $J < 1$ and a chaotic phase for $J > 1$. From Eq. (17) we can conclude that these two regimes correspond to qualitatively very different entropy production rates $\langle \dot{s}_{\text{tot}} \rangle$: in the disordered phase, $\langle \dot{s}_{\text{tot}} \rangle$ essentially settles on a finite value independent of the thermal noise strength; meanwhile, in the chaotic phase, $\langle \dot{s}_{\text{tot}} \rangle$ diverges as the noise becomes negligible. It is then natural to ask whether this transition is a genuine thermodynamic phase-transition. The framework of stochastic thermodynamics suggests that first-order phase-transition generally have a discontinuity in $\sigma^2 \langle \dot{s}_{\text{tot}} \rangle$, while higher order phase-transitions have a discontinuity in their derivatives with respect to J [55]. In Fig. 3, we observe that $\sigma^2 \langle \dot{s}_{\text{tot}} \rangle$ vanishes as $\sigma \rightarrow 0$ for $J < J_c$, whereas it continuously changes to a finite value for $J > J_c$. This indeed suggests a continuous transition, in agreement with the literature showing a smooth increase from zero of the largest Lyapunov exponent [56] and the critical slowing down [13] at the onset of chaos.

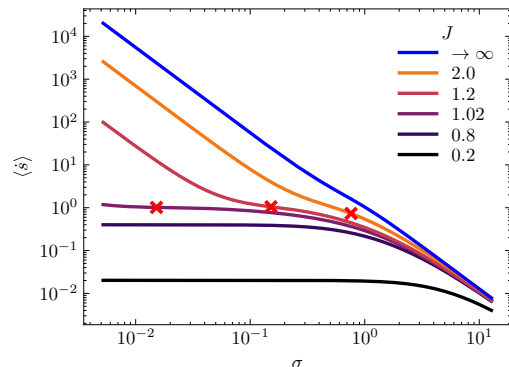


FIG. 4. Entropy production rate as function of σ below the transition to chaos $J = 0.2, 0.8$ and it $J = 1.02, 1.2, 2$ and $J \rightarrow \infty$ using the exact numerics of DMFT. The approximate critical point $\sigma = 3^{-1/4}(J - 1)$ are denoted with red crosses.

In Fig. 4, we show that the signatures of this phase-transition carry over to finite noise levels. One can verify that for $J < 1$ levels off at relatively high noise-levels ($\sigma \sim 10^{-1}$) and does no longer increase when σ decreases. For $J > 1$ on the other hand, one can see that there is an intermediate levelling off, but that the entropy production rate starts increasing again for $\sigma < 3^{-1/4}(J - 1)$, denoted by red crosses, corresponding to $J = J_c$. If one decreases the noise beyond this point, one observes that the entropy production rate starts scaling as σ^{-2} again.

Conclusions. In this paper, we study the entropy production rate in a random recurrent neural network that undergoes a transition from fixed-point to chaotic regime with increasing coupling heterogeneity. Crucially, our analysis is based on applying DMFT to the study of the system's entropy production rate. It is possible to apply this approach to more complex dynamics with multiple fixed points [57], suppression of chaos [58–60], structural chaos [61] and non-monotonic dependence on noise [62], or to study the entropy production rate in other types of networks such as sparse directed networks [63], deep neural networks [64, 65], networks with heterogeneous degree distribution [66–68], multiple populations [69–71], low-rank structures [72], or synaptic plasticity [11]. In particular, this might lead to design principles for minimizing the thermodynamic cost of operating a diverse set of neural networks.

Another interesting research direction would be to check whether the results from this letter can be extended to other chaotic systems, such as logistic maps [73], or active nematics [74]. In particular, it would be interesting to check whether one can find similar scaling of entropy production rate with noise in the chaotic phase. If so, this could lead to universal thermodynamic bounds and constraints at the onset of chaos – a first crucial step towards a general framework for quantifying non-equilibrium phase transition in chaotic systems.

Finally, of paramount importance is the question of finding an optimal protocol that minimizes the amount of heat necessary to drive a system towards its chaotic regime. This would require an extension of our analysis to systems with time-dependent driving. For this kind of problems, one could use the recently developed linear-response framework [75, 76].

Albert Alonso acknowledges support from the Novo Nordisk Foundation Grant Agreement NNF20OC0062047. Karel Proesmans is funded by the European Union’s Horizon 2020 research and innovation program under the Marie Skłodowska-Curie grant agreement No. 101064626 ‘TSBC’, and from the Novo Nordisk Foundation (grant No. NNF18SA0035142 and NNF21OC0071284). We would like to thank Carlos E. Fiore, Etienne Fodor, Samantha Fournier, Prashant Singh and Jonas Berx for stimulating discussions.

-
- [1] P. C. Martin, E. D. Siggia, and H. A. Rose, Statistical dynamics of classical systems, *Phys. Rev. A* **8**, 423 (1973).
- [2] C. De Dominicis and L. Peliti, Field-theory renormalization and critical dynamics above T_c : Helium, antiferromagnets, and liquid-gas systems, *Phys. Rev. B* **18**, 353 (1978).
- [3] A. Coolen, Statistical mechanics of recurrent neural networks II — Dynamics, in *Neuro-Informatics and Neural Modelling*, Handbook of Biological Physics, Vol. 4, edited by F. Moss and S. Gielen (North-Holland, 2001) pp. 619–684.
- [4] C. C. Chow and M. A. Buice, Path integral methods for stochastic differential equations, *J. Math. Neurosci.* **5**, 8 (2015).
- [5] J. A. Hertz, Y. Roudi, and P. Sollich, Path integral methods for the dynamics of stochastic and disordered systems, *Journal of Physics A: Mathematical and Theoretical* **50**, 033001 (2016).
- [6] D. Martí, N. Brunel, and S. Ostoic, Correlations between synapses in pairs of neurons slow down dynamics in randomly connected neural networks, *Phys. Rev. E* **97**, 062314 (2018).
- [7] L. F. Cugliandolo, Recent applications of dynamical mean-field methods, *Annual Review of Condensed Matter Physics* **15**, 177 (2024).
- [8] L. F. Cugliandolo and J. Kurchan, Analytical solution of the off-equilibrium dynamics of a long-range spin-glass model, *Phys. Rev. Lett.* **71**, 173 (1993).
- [9] M. Opper and S. Diederich, Phase transition and $1/f$ noise in a game dynamical model, *Phys. Rev. Lett.* **69**, 1616 (1992).
- [10] F. Mignacco and P. Urbani, The effective noise of stochastic gradient descent, *Journal of Statistical Mechanics: Theory and Experiment* **2022**, 083405 (2022).
- [11] D. G. Clark and L. F. Abbott, Theory of coupled neuronal-synaptic dynamics, *Phys. Rev. X* **14**, 021001 (2024).
- [12] C. Keup, T. Kühn, D. Dahmen, and M. Helias, Transient chaotic dimensionality expansion by recurrent networks, *Phys. Rev. X* **11**, 021064 (2021).
- [13] J. Schuecker, S. Goedeke, and M. Helias, Optimal sequence memory in driven random networks, *Phys. Rev. X* **8**, 041029 (2018).
- [14] F. Mastrogiuseppe and S. Ostoic, Intrinsically-generated fluctuating activity in excitatory-inhibitory networks, *PLOS Computational Biology* **13**, 1 (2017).
- [15] C. Martorell, R. Calvo, A. Annibale, and M. A. Muñoz, Dynamically selected steady states and criticality in non-reciprocal networks, *Chaos, Solitons & Fractals* **182**, 114809 (2024).
- [16] G. Bunin, Ecological communities with lotka-volterra dynamics, *Phys. Rev. E* **95**, 042414 (2017).
- [17] F. Roy, G. Biroli, G. Bunin, and C. Cammarota, Numerical implementation of dynamical mean field theory for disordered systems: application to the Lotka–Volterra model of ecosystems, *Journal of Physics A: Mathematical and Theoretical* **52**, 484001 (2019).
- [18] T. A. de Pirey and G. Bunin, Critical behavior of a phase transition in the dynamics of interacting populations (2024), arXiv:2402.05063 [cond-mat.stat-mech].
- [19] T. Galla, Generating-functional analysis of random lotka-volterra systems: A step-by-step guide (2024), arXiv:2405.14289 [cond-mat.dis-nn].
- [20] T. M. Pham and K. Kaneko, Dynamical theory for adaptive systems (2024), arXiv:2306.01403.
- [21] S. Shmakov and P. B. Littlewood, Coalescence of limit cycles in the presence of noise, *Phys. Rev. E* **109**, 024220 (2024).
- [22] A. Prüser, S. Rosmej, and A. Engel, Nature of the volcano transition in the fully disordered kuramoto model, *Phys. Rev. Lett.* **132**, 187201 (2024).
- [23] N. Silvano and D. G. Barci, Emergent gauge symmetry in active brownian matter, *Phys. Rev. E* **109**, 044605 (2024).
- [24] M. Paoluzzi, C. Maggi, and A. Crisanti, Statistical field theory and effective action method for scalar active matter, *Phys. Rev. Res.* **2**, 023207 (2020).
- [25] T. Agranov, M. E. Cates, and R. L. Jack, Entropy production and its large deviations in an active lattice gas, *Journal of Statistical Mechanics: Theory and Experiment* **2022**, 123201 (2022).
- [26] F. Ferretti, S. Grosse-Holz, C. Holmes, J. L. Shivers, I. Giardina, T. Mora, and A. M. Walczak, Signatures of irreversibility in microscopic models of flocking, *Phys. Rev. E* **106**, 034608 (2022).
- [27] Q. Yu and Y. Tu, Energy cost for flocking of active spins: The cusped dissipation maximum at the flocking transition, *Phys. Rev. Lett.* **129**, 278001 (2022).
- [28] T. GrandPre, K. Klymko, K. K. Mandadapu, and D. T. Limmer, Entropy production fluctuations encode collective behavior in active matter, *Phys. Rev. E* **103**, 012613 (2021).
- [29] H. Alston, L. Cocconi, and T. Bertrand, Irreversibility across a nonreciprocal \mathcal{PT} -symmetry-breaking phase transition, *Phys. Rev. Lett.* **131**, 258301 (2023).
- [30] T. Tomé and M. J. de Oliveira, Entropy production in nonequilibrium systems at stationary states, *Phys. Rev. Lett.* **108**, 020601 (2012).
- [31] C. E. F. Noa, P. E. Harunari, M. J. de Oliveira, and C. E. Fiore, Entropy production as a tool for characterizing nonequilibrium phase transitions, *Phys. Rev. E* **100**, 012104 (2019).
- [32] T. Martynek, S. H. L. Klapp, and S. A. M. Loos, Entropy production at criticality in a nonequilibrium potts model,

- New Journal of Physics **22**, 093069 (2020).
- [33] T. Tomé, C. E. Fiore, and M. J. de Oliveira, Stochastic thermodynamics of opinion dynamics models, *Phys. Rev. E* **107**, 064135 (2023).
- [34] I. V. Oliveira, C. Wang, G. Dong, R. Du, C. E. Fiore, A. L. Vilela, and H. E. Stanley, Entropy production on cooperative opinion dynamics, *Chaos, Solitons & Fractals* **181**, 114694 (2024).
- [35] D. Zhang, Y. Cao, Q. Ouyang, and Y. Tu, The energy cost and optimal design for synchronization of coupled molecular oscillators, *Nature Physics* **16**, 95 (2020).
- [36] J. H. Fritz, B. Nguyen, and U. Seifert, Stochastic thermodynamics of chemical reactions coupled to finite reservoirs: A case study for the brusselator, *The Journal of Chemical Physics* **152** (2020).
- [37] T. Herpich, J. Thingna, and M. Esposito, Collective power: Minimal model for thermodynamics of nonequilibrium phase transitions, *Phys. Rev. X* **8**, 031056 (2018).
- [38] G. Falasco, R. Rao, and M. Esposito, Information thermodynamics of turing patterns, *Physical review letters* **121**, 108301 (2018).
- [39] S. Rana and A. C. Barato, Precision and dissipation of a stochastic turing pattern, *Physical Review E* **102**, 032135 (2020).
- [40] M. Aguilera, M. Igarashi, and H. Shimazaki, Nonequilibrium thermodynamics of the asymmetric Sherrington-Kirkpatrick model, *Nature Communications* **14**, 3685 (2023).
- [41] A. C. Barato and U. Seifert, Thermodynamic uncertainty relation for biomolecular processes, *Physical review letters* **114**, 158101 (2015).
- [42] J. M. Horowitz and T. R. Gingrich, Thermodynamic uncertainty relations constrain non-equilibrium fluctuations, *Nature Physics* **16**, 15 (2020).
- [43] E. Aurell, C. Mejía-Monasterio, and P. Muratore-Ginanneschi, Optimal protocols and optimal transport in stochastic thermodynamics, *Physical review letters* **106**, 250601 (2011).
- [44] T. Van Vu and K. Saito, Thermodynamic unification of optimal transport: Thermodynamic uncertainty relation, minimum dissipation, and thermodynamic speed limits, *Physical Review X* **13**, 011013 (2023).
- [45] M. A. Buice and C. C. Chow, Beyond mean field theory: statistical field theory for neural networks, *Journal of Statistical Mechanics: Theory and Experiment* **2013**, P03003 (2013).
- [46] H. Jaeger and H. Haas, Harnessing nonlinearity: Predicting chaotic systems and saving energy in wireless communication, *Science* **304**, 78 (2004).
- [47] H. Sompolinsky, A. Crisanti, and H. J. Sommers, Chaos in random neural networks, *Phys. Rev. Lett.* **61**, 259 (1988).
- [48] A. Crisanti and H. Sompolinsky, Path integral approach to random neural networks, *Phys. Rev. E* **98**, 062120 (2018).
- [49] T. Cabana and J. Touboul, Large deviations, dynamics and phase transitions in large stochastic and disordered neural networks, *Journal of Statistical Physics* **153**, 211 (2013).
- [50] J. MacLaurin, M. Silverstein, and P. Vilanova, Population level activity in large random neural networks, *arXiv* **2401.15272** (2024).
- [51] T. Toyozumi and L. F. Abbott, Beyond the edge of chaos: Amplification and temporal integration by recurrent networks in the chaotic regime, *Phys. Rev. E* **84**, 051908 (2011).
- [52] D. Sussillo and L. Abbott, Generating coherent patterns of activity from chaotic neural networks, *Neuron* **63**, 544 (2009).
- [53] A. Ingrosso and E. Panizon, Machine learning at the mesoscale: A computation-dissipation bottleneck, *Phys. Rev. E* **109**, 014132 (2024).
- [54] U. Seifert, Stochastic thermodynamics, fluctuation theorems and molecular machines, *Reports on progress in physics* **75**, 126001 (2012).
- [55] B. Nguyen and U. Seifert, Exponential volume dependence of entropy-current fluctuations at first-order phase transitions in chemical reaction networks, *Physical Review E* **102**, 022101 (2020).
- [56] R. Engelken, F. Wolf, and L. F. Abbott, Lyapunov spectra of chaotic recurrent neural networks, *Phys. Rev. Res.* **5**, 043044 (2023).
- [57] J. Breffle, S. Mokashe, S. Qiu, and P. Miller, Multistability in neural systems with random cross-connections, *Biological Cybernetics* (2023).
- [58] K. Rajan, L. F. Abbott, and H. Sompolinsky, Stimulus-dependent suppression of chaos in recurrent neural networks, *Phys. Rev. E* **82**, 011903 (2010).
- [59] R. Engelken, A. Ingrosso, R. Khajeh, S. Goedeke, and L. F. Abbott, Input correlations impede suppression of chaos and learning in balanced firing-rate networks, *PLOS Computational Biology* **18**, 1 (2022).
- [60] S. Takasu and T. Aoyagi, Suppression of chaos in a partially driven recurrent neural network, *Phys. Rev. Res.* **6**, 013172 (2024).
- [61] F. Mastrogiuseppe and S. Ostojic, Linking connectivity, dynamics, and computations in low-rank recurrent neural networks, *Neuron* **99**, 609 (2018).
- [62] J. Garnier-Brun, M. Benzaquen, and J.-P. Bouchaud, Unlearnable games and “satisficing” decisions: A simple model for a complex world, *Phys. Rev. X* **14**, 021039 (2024).
- [63] F. L. Metz, Dynamical mean-field theory of complex systems on sparse directed networks (2024), *arXiv:2406.06346*.
- [64] Y. Bahri, J. Kadmon, J. Pennington, S. S. Schoenholz, J. Sohl-Dickstein, and S. Ganguli, Statistical mechanics of deep learning, *Annual Review of Condensed Matter Physics* **11**, 501 (2020).
- [65] K. Segadlo, B. Epping, A. van Meegen, D. Dahmen, M. Krämer, and M. Helias, Unified field theoretical approach to deep and recurrent neuronal networks, *Journal of Statistical Mechanics: Theory and Experiment* **2022**, 103401 (2022).
- [66] F. Aguirre-López, Heterogeneous mean-field analysis of the generalized lotka-volterra model on a network, *arXiv* **2404.11164** (2024).
- [67] J. I. Park, D.-S. Lee, S. H. Lee, and H. J. Park, Incorporating heterogeneous interactions for ecological biodiversity, *arXiv* **2403.15730** (2024).
- [68] L. Poley, T. Galla, and J. W. Baron, Interaction networks in persistent lotka-volterra communities, *arXiv* **2404.08600** (2024).
- [69] J. Kadmon and H. Sompolinsky, Transition to chaos in random neuronal networks, *Phys. Rev. X* **5**, 041030 (2015).
- [70] J. Aljadeff, M. Stern, and T. Sharpee, Transition to chaos in random networks with cell-type-specific connectivity,

- Phys. Rev. Lett. **114**, 088101 (2015).
- [71] I. D. Landau and H. Sompolinsky, Macroscopic fluctuations emerge in balanced networks with incomplete recurrent alignment, *Phys. Rev. Res.* **3**, 023171 (2021).
- [72] F. Schuessler, A. Dubreuil, F. Mastrogiuseppe, S. Ostojic, and O. Barak, Dynamics of random recurrent networks with correlated low-rank structure, *Phys. Rev. Res.* **2**, 013111 (2020).
- [73] F. Baldovin and A. Robledo, Parallels between the dynamics at the noise-perturbed onset of chaos in logistic maps and the dynamics of glass formation, *Physical Review E—Statistical, Nonlinear, and Soft Matter Physics* **72**, 066213 (2005).
- [74] V. Venkatesh, C. Mondal, and A. Doostmohammadi, Distinct impacts of polar and nematic self-propulsion on active unjamming, *The Journal of Chemical Physics* **157** (2022).
- [75] D. A. Sivak and G. E. Crooks, Thermodynamic metrics and optimal paths, *Physical review letters* **108**, 190602 (2012).
- [76] L. K. Davis, K. Proesmans, and É. Fodor, Active matter under control: Insights from response theory, *Physical Review X* **14**, 011012 (2024).

APPENDIX A: DERIVATION OF EQ. (5) AND EQ. (10)

Following the standard presentation in [3–6, 45], we derive DMFT for a *quenched* ensemble of random matrices in Eq. (2). Let $\langle \cdot \rangle$ in this section denote the average taken with respect to the measure $\mathbb{P}(\{\mathbf{x}\}_{0,t_f})$ – the distribution of an ensemble of trajectories $\{\mathbf{x}\}_{0,t_f}$, from $\mathbf{x}_0 = \mathbf{x}(0)$ at $t = 0$ to $\mathbf{x}_f = \mathbf{x}(t_f)$ at $t = t_f$. We shall assume that the system is in steady state and therefore take $P(\mathbf{x}(0))$ as the steady-state distribution.

The probability to observe a trajectory $\{\mathbf{x}\}_{0,t_f}$ is then given by

$$\mathbb{P}(\{\mathbf{x}\}_{0,t_f}) = \int D[\hat{x}f\hat{f}] \exp \left\{ i \sum_{k=1}^N \int dt \left[S_k^{(0)} - \sum_{j=1}^N J_{kj} \hat{f}_k x_j \right] \right\} \quad (18)$$

where $D[\hat{x}f\hat{f}] := \prod_{t=0}^{t_f} \prod_{k=1}^N D\hat{x}_k(t) Df_k(t) D\hat{f}_k(t)$ is the functional measure over all possible paths, and where

$$S_k^{(0)}(t) = \hat{x}_k \left[(\partial_t + 1)x_k(t) - \tanh(f_k(t)) \right] + i\sigma^2 \hat{x}_k^2(t)/2 + \hat{f}_k(t)f_k(t) \quad (19)$$

is the free Lagrangian for a neuron k . Using the definition, Eq. (9), one can immediately see that

$$Z_S[\lambda] = \left[\int D[x\hat{x}f\hat{f}] \exp \left\{ \Omega - i \sum_{j \neq k}^N J_{kj} \int dt \hat{f}_k x_j \right\} \right]_{\mathbf{J}} \quad (20)$$

with

$$\Omega = i \sum_{k=1}^N \int dt \left[S_k^{(0)} + \lambda(t) \dot{x}_k(t) [\tanh(f_k(t)) - x_k(t)] \right]. \quad (21)$$

To make further progress, we will now explicitly take the average over \mathbf{J} . Firstly, we note that only the last term in the exponential of Eq. (20) depends on \mathbf{J} and that the distribution of \mathbf{J} is Gaussian with covariances given by Eq. (2). This can be used to get

$$\begin{aligned} Z_S[\lambda] &= \int D[x\hat{x}f\hat{f}] \exp \{ \Omega \} \left[\exp \left\{ -i \sum_{j \neq k}^N J_{kj} \int dt \hat{f}_k x_j \right\} \right]_{\mathbf{J}} \\ &= \int D[x\hat{x}f\hat{f}] \exp \left\{ \Omega - \frac{J^2}{2N} \int dt dt' \sum_{j \neq k}^N A_{kj}(t, t') \right\} \end{aligned} \quad (22)$$

where

$$A_{kj}(t, t') = \hat{f}_k(t) \hat{f}_k(t') x_j(t) x_j(t') \quad (23)$$

We now introduce new observables:

$$q(t, t') = \frac{1}{N} \sum_k x_k(t) x_k(t') \quad (24a)$$

$$Q(t, t') = \frac{1}{N} \sum_k \hat{f}_k(t) \hat{f}_k(t'). \quad (24b)$$

These definitions can be used to write

$$\begin{aligned} Z_S[\lambda] &= \int D[x\hat{x}f\hat{f}] \int D[Qq] \exp \left\{ \Omega - \frac{NJ^2}{2} \int dt dt' q(t, t') Q(t, t') \right\} \delta \left(Nq(t, t') - \sum_k x_k(t) x_k(t') \right) \\ &\quad \times \delta \left(NQ(t, t') - \sum_k \hat{f}_k(t) \hat{f}_k(t') \right) \end{aligned} \quad (25)$$

where $D[Qq] = Dq(t, t')DQ(t, t')/N^2$. We can now use the identity

$$\delta \left(Nq - \sum_k x_k(t)x_k(t') \right) = \frac{1}{2\pi} \int d\hat{q} e^{i \int dt \int dt' \hat{q}(t, t') (Nq(t, t') - \sum_k x_k(t)x_k(t'))} \quad (26)$$

to write

$$Z_S[\lambda] = \int D[Q\hat{Q}q\hat{q}] \exp \left\{ N \left(g(q, \hat{q}, Q, \hat{Q}) + \frac{1}{N} \log \int D[x\hat{x}f\hat{f}] \exp \left(\mathcal{L}(x, \hat{x}, f, \hat{f}, \hat{q}, \hat{Q}) \right) \right) \right\}, \quad (27)$$

with $D[Q\hat{Q}q\hat{q}] = D[Qq]D\hat{q}(t, t')D\hat{Q}(t, t')/(4\pi^2)$,

$$g(q, \hat{q}, Q, \hat{Q}) = i \int dt dt' [\hat{q}q + \hat{Q}Q] - \frac{J^2}{2} \int dt dt' qQ \quad (28)$$

$$\mathcal{L}(x, \hat{x}, f, \hat{f}, \hat{q}, \hat{Q}) = \Omega - i \sum_k \int dt dt' [\hat{q}(t, t')x_k(t)x_k(t') + \hat{Q}(t, t')\hat{f}_k(t)\hat{f}_k(t')]. \quad (29)$$

Up to this points, all calculations have been exact and we have not done any approximations. To make further progress, we will now do a mean-field approximation. In particular, we note that for large N the integral in Eq. (25) is completely dominated by values for which the term inside the exponential is maximized. Therefore, we can do a saddle-point approximation [5], to arrive at

$$Z_S[\lambda] \underset{N \rightarrow \infty}{=} Z_S^{(MF)}[\lambda] = \max_{q, \hat{q}, Q, \hat{Q}} \exp \left\{ N \left(g(q, \hat{q}, Q, \hat{Q}) + \frac{1}{N} \log \int D[x\hat{x}f\hat{f}] \exp \left(\mathcal{L}(x, \hat{x}, f, \hat{f}, \hat{q}, \hat{Q}) \right) \right) \right\} \quad (30)$$

One can now take the derivatives with respect to q, \hat{q}, Q and \hat{Q} to find their optimal values. This gives

$$\hat{q}(t, t') = -\frac{iJ^2}{2} Q(t, t') \quad (31)$$

$$\hat{Q}(t, t') = -\frac{iJ^2}{2} q(t, t') \quad (32)$$

$$q(t, t') = \frac{1}{N} \sum_k \langle x_k(t)x_k(t') \rangle_{\mathcal{L}} \quad (33)$$

$$Q(t, t') = \frac{1}{N} \sum_k \langle \hat{f}_k(t)\hat{f}_k(t') \rangle_{\mathcal{L}}, \quad (34)$$

where

$$\langle X \rangle_{\mathcal{L}} = \frac{\int D[x\hat{x}f\hat{f}] X(x, \hat{x}, f, \hat{f}) \exp \left(\mathcal{L}(x, \hat{x}, f, \hat{f}, \hat{q}, \hat{Q}) \right)}{\int D[x\hat{x}f\hat{f}] \exp \left(\mathcal{L}(x, \hat{x}, f, \hat{f}, \hat{q}, \hat{Q}) \right)} \quad (35)$$

for any observable X . This means that the moment-generating function can be written as

$$Z_S^{(MF)} = \int D[x\hat{x}f\hat{f}] \exp \left(\frac{NJ^2}{2} \int dt dt' q(t, t')Q(t, t') + i \sum_k \int dt \left[S_k^{(0)}(t) + \lambda(t)\dot{x}_k(t) \{ \tanh(f_k(t)) - x_k(t) \} \right] \right. \\ \left. - \frac{J^2}{2} \int dt dt' \left[Q(t, t')x_k(t)x_k(t') + q(t, t')\hat{f}_k(t)\hat{f}_k(t') \right] \right). \quad (36)$$

One can now see that all neurons k and k' are independent of each other. Therefore, this can be rewritten as

$$Z_S^{(MF)} = \left(\int D[x\hat{x}f\hat{f}] \exp \left\{ i \int dt \left[S^{(0)}(t) + \lambda(t)\dot{x}(t) \{ \tanh(f(t)) - x(t) \} \right] \right. \right. \\ \left. \left. + \frac{J^2}{2} \int dt dt' \left[Q(t, t')(q(t, t') - x(t)x(t')) - q(t, t')\hat{f}(t)\hat{f}(t') \right] \right\} \right)^N, \quad (37)$$

where we replaced the N -dimensional vector \mathbf{x} by a single neuron x and similar for \hat{x} , f , \hat{f} . Before continuing, we note that, for $\lambda = 0$, $q(t, t')$ and $Q(t, t')$ have solutions given by

$$q(t, t') = \langle x(t)x(t') \rangle^{(MF)}, \quad Q(t, t') = \langle \hat{f}(t)\hat{f}(t') \rangle^{(MF)}. \quad (38)$$

Here, the superscript (MF) stands for the average taken over the probability distribution

$$\mathbb{P}(\{x\}_{0,t_f}, \{f\}_{0,t_f}) = \int D[\hat{x}, \hat{f}] \exp \left(i \int dt S^{(0)}(t) - \frac{1}{2} \int dt dt' q(t, t') \hat{f}(t) \hat{f}(t') \right). \quad (39)$$

One can easily verify that these relations are indeed a self-consistent solution of Eqs. (33)-(34). We can use the normalisation condition [19] to further obtain, again for $\lambda = 0$:

$$\langle \hat{f}(t)\hat{f}(t') \rangle^{(MF)} = 0 \Rightarrow Q(t, t') = 0 \quad (40)$$

Furthermore, we note that integrating out the field $\{f\}$ in the joint distribution, Eq. (39) we obtain

$$\mathbb{P}(\{x\}_{0,t_f}) = \int D\hat{x} \exp \left(\hat{x}(t) \left[(\partial_t + 1)x(t) - \tanh(\eta(t)) \right] + i\sigma^2 \hat{x}_k^2(t)/2 \right) \quad (41)$$

which corresponds to the path measure of the effective dynamics in Eqs. (5)-(7)

One can now use the definition of the moment generating function to show that

$$\begin{aligned} \langle \dot{S}^{\text{res}}(t) \rangle &= \frac{1}{i} \frac{\delta}{\delta \lambda(t)} Z_S^{(MF)}[\lambda] \Big|_{\lambda=0} \\ &= N \left(\langle \dot{x}(t) \circ [\tanh(f(t)) - x(t)] \rangle^{(MF)} + \frac{J^2}{2} \frac{\delta}{\delta \lambda(t)} \int dt' \int dt'' q(t, t') Q(t, t') \right) \Big|_{\lambda=0} \\ &\quad - \frac{NJ^2}{2} \left(\int dt' \int dt'' \left(\frac{\delta}{\delta \lambda(t)} Q(t', t'') \langle x(t')x(t'') \rangle^{(MF)} + \frac{\delta}{\delta \lambda(t)} q(t, t') \langle \hat{f}(t)\hat{f}(t') \rangle^{(MF)} \right) \right) \Big|_{\lambda=0} \\ &= N \langle \dot{x}(t) \circ [\tanh(f(t)) - x(t)] \rangle^{(MF)}, \end{aligned} \quad (42)$$

where we used Eq. (38) and the fact that $\langle \hat{f}(t)\hat{f}(t') \rangle^{(MF)}$ to arrive at the last line. This completes the proof.

APPENDIX B: DERIVATION OF EQ. (11)

To compute the averaged entropy production rate we start from the definition and assume steady-state to find

$$\begin{aligned} \langle \dot{s}^{(MF)} \rangle &\equiv \frac{1}{i} \frac{\partial}{\partial \lambda(t)} Z_S[\lambda] \Big|_{\lambda=0} \\ &= \frac{2}{\sigma^2} \langle \dot{x}(t) \times [\tanh(\eta(t)) - x(t)] \rangle \\ &= \frac{2}{\sigma^2} \frac{d}{d\tau} C_{ux}(\tau) \Big|_{\tau=0} \end{aligned} \quad (43)$$

On the other hand, one can solve Eq. (5) to find

$$x(t) = \int_0^\infty d\tau e^{-\tau} (\xi(t - \tau) + u(t - \tau)) \quad (44)$$

Due to the steady state assumption, one can use this to write

$$\begin{aligned} \frac{d^2}{dt^2} C_x(t) &= \frac{d^2}{dt^2} \int_0^\infty d\tau \int_0^\infty d\tau' e^{-\tau-\tau'} (\langle \xi(-\tau)\xi(t - \tau') \rangle + \langle u(-\tau)u(t - \tau') \rangle) \\ &= \frac{d}{dt} \int_0^\infty d\tau \int_0^\infty d\tau' e^{-\tau-\tau'} \frac{d}{d\tau} (\langle \xi(0)\xi(t - \tau' + \tau) \rangle + \langle u(0)u(t - \tau' + \tau) \rangle) \\ &= \frac{d}{dt} \int_0^\infty d\tau' e^{-\tau'} (\langle \xi(0)\xi(t - \tau') \rangle + \langle u(0)u(t - \tau') \rangle) - \frac{d}{dt} C_x(t) \\ &= \sigma^2 \frac{d}{dt} e^{-t} + \frac{d}{dt} C_{ux}(t) - \frac{d}{dt} C_x(t) \end{aligned} \quad (45)$$

where we used

$$\frac{d}{dt}C_{ux}(t) = \frac{d}{dt} \int_0^\infty d\tau e^{-\tau} (\langle u(0)\xi(-(-t-\tau)) \rangle + \langle u(0)u(t-\tau) \rangle)$$

to arrive at the last line. We can now use Eq. (15) to find

$$\left. \frac{d}{dt}C_{ux}(t) \right|_{t=0} = \left. \frac{d^2}{dt^2}C_x(t) \right|_{t=0} - \frac{\sigma^2}{2}. \quad (46)$$

Plugging this in into Eq. (43) immediately leads to Eq. (11)

APPENDIX C: DERIVATIONS OF EQS. (13)-(15)

Firstly, we note that by multiplying the DMFT equation by itself, one can get

$$(\partial_t + 1)x(t)(\partial_{t'} + 1)x(t') = (u(t) + \xi(t))(u(t') + \xi(t')) \quad (47)$$

Taking the average of this equation under steady-state and using time-translation invariance to write $\tau = t - t'$, one can rewrite this equation to

$$-\partial_\tau^2 C_x(\tau) + C_x(\tau) = \langle \tanh(\eta(\tau)) \tanh(\eta(0)) \rangle_\eta + \sigma^2 \delta(\tau). \quad (48)$$

One can then use Price's theorem to show that

$$\frac{\partial}{\partial C_x(\tau)} \langle \Omega(\eta(\tau)) \Omega(\eta(0)) \rangle_\eta = J^2 \langle \tanh(\eta(\tau)) \tanh(\eta(0)) \rangle_\eta. \quad (49)$$

Combining these two equations leads to Eqs. (13).

To derive the boundary conditions, we first note that Eq. (13) corresponds to the Euler-Lagrange equation of the following Lagrangian for $t > 0$:

$$\mathcal{L} = \frac{\dot{C}_x(t)}{2} - V(C_x(t)|C_x(0)). \quad (50)$$

One can then use methods from analytical mechanics to show that

$$E = \frac{\dot{C}_x(t)^2}{2} + V(C_x(t)|C_x(0)) \quad (51)$$

is a constant of motion. We know on physical grounds that

$$\lim_{t \rightarrow \infty} C_x(t) = \lim_{t \rightarrow \infty} \dot{C}_x(t) = 0, \quad (52)$$

and that $V(0|C_0) = 0$. Combining these equations leads to

$$\frac{\dot{C}_x(0^+)^2}{2} + V(C_x(t)|C_x(0)) = 0. \quad (53)$$

Secondly, we note that, due to time-translation symmetry, one has

$$\dot{C}_x(0^+) = -\dot{C}_x(0^-). \quad (54)$$

This can only satisfy the first line of Eq. (13) if

$$\dot{C}_x(0^+) = -\frac{\sigma^2}{2}. \quad (55)$$

Combining this with Eq. (53) gives the initial conditions Eq. (15).

APPENDIX D: ASYMPTOTICS OF THE ENTROPY PRODUCTION

In this section, we will derive the asymptotics of the entropy production, as given in Eq. (17). To do this, we will first show that

$$V(C_x(t)|C_x(0)) \approx \begin{cases} \frac{(J^2-1)C_x(t)^2}{2} & J \ll 1 \\ C_x(t)^4 - \frac{(J-1)^2}{6}C_x(t)^2 & 0 < J - J_c \ll 1 \\ \frac{8(\sqrt{C_0^2 - C_x(t)^2} - C_0^2) + \pi C_x(t) - 2\pi C_x(t)^2 + 2C_x(t) \left(3 \tan^{-1} \left(\frac{\sqrt{C_x(t)^2 - C_0^2}}{C_x(t)} \right) - \tan^{-1} \left(\frac{C_x(t)}{\sqrt{C_x(t)^2 - C_0^2}} \right) \right)}{8\pi}} & J \gg 1 \end{cases} \quad (56)$$

One can then use the boundary condition, Eq. (16), to show that

$$C_x(0) \approx \begin{cases} \frac{\sigma^2}{2\sqrt{1-J^2}} & J \ll 1 \\ \left[\frac{(J-1)^2}{2} + \frac{1}{2} \sqrt{(J-1)^4 - 3\sigma^4} \right]^{1/2} & 0 < J - J_c \ll 1 \\ 1 - \frac{2}{\pi} + \sqrt{\left(1 - \frac{2}{\pi}\right)^2 + \frac{\sigma^4}{2}} & J - J_c \gg 1 \end{cases} \quad (57)$$

One can then plug this in into Eq. (16) to arrive at the final expressions, Eq. (17). The remainder of this section focusses on the derivation of Eq. (56) in the three different regimes.

$J \ll 1$

In the limit $J \ll 1$, the (co)variance associated with η will generally become small and therefore the behavior of $\Omega(\eta(t))$ only becomes important around 0, where one can do a lowest-order Taylor expansion,

$$\Omega(\eta(t)) = \frac{\eta(t)^2}{2} + O(\eta(t)^4) \quad (58)$$

Therefore, we can write

$$\begin{aligned} \langle \Omega(\eta(0))\Omega(\eta(t)) \rangle - \langle \Omega(\eta(0)) \rangle \langle \Omega(\eta(t)) \rangle &\approx \frac{\langle \eta(0)^2\eta(t)^2 \rangle - \langle \eta(0)^2 \rangle^2}{4} \\ &= \frac{J^4 C_x(t)^2}{2}, \end{aligned} \quad (59)$$

where we used the fact that the distribution is Gaussian to arrive at the second line. Plugging this into the definition of the potential, Eq. (13) immediately leads to the first line of Eq. (56).

$0 < J - J_c \ll 1$ and $\sigma \ll 1$

It can be shown that in the limit $\sigma = 0$ and $J \leq 1$ one has $C(t) = 0$ for all t . Therefore, we can assume in this section that $C(t)$ is small and we can expand

$$\Omega(\eta(t)) \simeq \frac{\eta(t)^2}{2} - \frac{\eta(t)^4}{12} + \frac{\eta(t)^6}{45} + O(\eta(t)^8). \quad (60)$$

This leads to

$$\langle \Omega(\eta(0))\Omega(\eta(t)) \rangle \simeq \frac{\langle \eta(0)^2\eta(t)^2 \rangle}{4} - \frac{\langle \eta(0)^2\eta(t)^4 \rangle}{12} + \frac{\langle \eta(0)^4\eta(t)^4 \rangle}{144} + \frac{\langle \eta(0)^2\eta(t)^6 \rangle}{45} \quad (61)$$

$$= \frac{J^6}{6}C(t)^4 + \left(\frac{5}{2}J^6C_0^2 - J^4C_0 + \frac{J^2}{2} \right) C(t)^2, \quad (62)$$

where we used the Gaussianity of the distribution. One can use this to show that

$$V(C_0|C_0) \simeq \frac{8}{3}J^6C_0^4 - J^4C_0^3 + \frac{(J^2-1)}{2}C_0^2. \quad (63)$$

In the limit of zero noise, this means that

$$\frac{8}{3}J^6C_0^4 - J^4C_0^3 + \frac{(J^2 - 1)}{2}C_0^2 \simeq 0 \quad (64)$$

or

$$\begin{aligned} C_0 &\simeq \frac{3}{16J^3} \left(J - \sqrt{\frac{16 - 13J^2}{3}} \right) \\ &= (J - 1) - \frac{5}{6}(J - 1)^2 + O((J - 1)^3), \end{aligned} \quad (65)$$

where we did a Taylor expansion around $J = 1$ in the second line. Plugging this back in into Eq. (62) and doing a lowest order expansion leads to

$$V(C|C_0) \simeq \frac{C^4}{6} - \frac{(J - 1)^2}{6} C^2 \quad (66)$$

If we now use this equation of V as an approximation for small but finite σ , we get the following boundary condition:

$$\frac{C_0^4}{6} - \frac{(J - 1)^2}{6} C_0^2 + \frac{\sigma^4}{8} = 0 \quad (67)$$

Solving this equation for C_0 , we obtain the physical solution

$$C_0 = \left[\frac{(J - 1)^2}{2} + \frac{1}{2} \sqrt{(J - 1)^4 - 3\sigma^4} \right]^{1/2} \quad (68)$$

In the small noise regime, for $J - J_c < 0.1$ the autocorrelation C_0 derived from our approximation agrees well with what can be obtained from the numerical solution of the self-consistency equation Eq. (15). However, as long as $J - J_c$ gets larger, our approximation in Eq. (68) overestimates the true value of $C_x(0)$, resulting in an overestimation of the entropy production rate.

$J \gg 1$

In the limit $J \gg 1$ the variance of $\eta(t)$ diverges and therefore the averages of $\Omega(\eta(t))$ are dominated by their tails, where one can approximate

$$\Omega(\eta(t)) \approx |\eta(t)| - \ln 2. \quad (69)$$

Therefore,

$$\begin{aligned} \langle \Omega(\eta(0))\Omega(\eta(t)) \rangle - \langle \Omega(\eta(0)) \rangle \langle \Omega(\eta(t)) \rangle &\approx \langle |\eta(0)| |\eta(t)| \rangle - \langle |\eta(0)| \rangle^2 \\ &= \frac{8(\sqrt{C_0^2 - C_x(t)^2} - C_0^2) + \pi C_x(t)}{8\pi J^2} \\ &\quad + \frac{C_x(t) \left(3 \tan^{-1} \left(\frac{\sqrt{C_x(t)^2 - C_0^2}}{C_x(t)} \right) - \tan^{-1} \left(\frac{C_x(t)}{\sqrt{C_x(t)^2 - C_0^2}} \right) \right)}{4\pi J^2}, \end{aligned} \quad (70)$$

Plugging this into the definition of the potential, Eq. (13) immediately leads to the last line of Eq. (56).